

Detecting hyperbolic geometry in networks: why triangles are not enough

Riccardo Michielan, Nelly Litvak, and Clara Stegehuis

Faculty of Electrical Engineering, Mathematics and Computer Science, University of Twente

(Dated: November 8, 2022)

In the past decade, geometric network models have received vast attention in the literature. These models formalize the natural idea that similar vertices are likely to connect. Because of that, these models are able to adequately capture many common structural properties of real-world networks, such as scale invariance and high clustering. Indeed, many real-world networks can be accurately modeled by positioning vertices of a network graph in hyperbolic spaces. Nevertheless, if one observes only the network connections, the presence of geometry is not always evident. Currently, triangle counts and clustering coefficients are the standard statistics to signal the presence of geometry. In this paper we show that triangle counts or clustering coefficients are insufficient because they fail to detect geometry induced by hyperbolic spaces. We therefore introduce a novel statistic, *weighted triangles*, which weighs triangles based on their evidence for geometry. We show analytically, as well as on synthetic and real-world data, that weighted triangles are a powerful statistic to detect hyperbolic geometry in networks.

I. INTRODUCTION

Network geometry is one of the most important features of real-world networks [1], as it explains frequently observed network properties, including scale-invariance, high clustering, and overlapping community structures. The concept of geometry is intimately connected to the idea of similarity in networks, that two similar vertices are likely to connect. Typical examples are social networks, where people sharing the same interests or living in the same region are more likely to interact, or the world wide web, where webpages sharing similar contents are often linked. The similarity of vertices can be modeled through geometry in a random graph. More specifically, two individuals can be modeled as vertices in a geometric space, and their similarity is then associated with a small distance between them. This class of models is often called geometric network models.

In the past decades, several geometric models have been introduced, aiming to model and understand real network properties [2–5]. The simplest example of geometric models are the random geometric graphs [6, 7], where an underlying Euclidean space is fixed, and nodes within a given radius are connected. However, random geometric graphs fail to describe the typical scale-free nature of real-world networks, where many nodes of low degree coexist with a few nodes of extremely large degrees. Instead, the hyperbolic space has been found to be extremely useful for modeling real-world networks [2], as it explains the heavy-tailed degree distributions that many networks possess, their efficient routing [8, 9] and their community structures [10]. Interestingly, the hyperbolic model is equivalent to the renowned \mathbb{S}^1 model, where nodes are uniformly distributed on the circle, and a soft constraint is assigned to the degrees [5]. Recently, a very intuitive network model called geometric inhomogeneous random graph (GIRG) has been proposed as a generalization of hyperbolic random graphs [3]. GIRGs combine the essential real-world properties of the hyperbolic

random graph with simpler mathematical formulations that make them mathematically more tractable than hyperbolic random graphs. In these models each vertex is positioned in a geometric space, and has a weight representing its ability to attract connections. Then, the probability of a connection between two vertices in the GIRG is an increasing function of the weight of each vertex, and a decreasing function of a distance between them.

Although in many cases network geometry is a natural assumption, networks may not be directly endowed with a metric space, and in principle they could also not possess any kind of geometry. Determining whether a given network has an underlying latent hyperbolic geometric space has been highlighted as a major open problem [1, 11]. Indeed, usually we can only observe the network connections, and not the network features which can cause geometry. The main question is then: can we assess whether these connections were formed by some underlying geometry?

It has often been assumed that high clustering, or a large amount of triangles, implies the presence of geometry [12]. Intuitively, in a geometric space, the triangle inequality ensures that two neighbors of a vertex are likely to be close to each other, and therefore likely to be connected. In fact, triangles are a powerful statistic to distinguish geometric and non-geometric networks, when assuming that the former can be endowed with an Euclidean space [13–15]. In this paper however, we show that pure triangle counts, as well as the average clustering coefficient, have limitations in detecting geometry induced by hyperbolic spaces. In fact, network models without any source of geometry may contain the same amount of triangles as hyperbolic random graphs, and may have arbitrary large average clustering coefficients. This is essentially due to the trade-off between weights and geometry in the GIRG representation of the hyperbolic model: connections can either be formed between high-weight nodes, or between close-by nodes. When the degree distribution has a particularly heavy tail, this

trade-off favors triangles formed by high weighted vertices. Therefore, the underlying geometry cannot always be detected by triangle counts or clustering coefficients.

In this work we develop a novel and powerful statistic called *weighted triangles* to detect hyperbolic geometry in networks, where triangles are weighted based on how likely they are to be caused by geometry. Triangles that carry low evidence for geometry are discounted, so that our statistic is able to differentiate hyperbolic geometry from non-geometric networks in a regime where standard triangle counts or clustering coefficients are not [16, 17]. We also provide experimental evidence that weighted triangles can successfully detect a geometric nature of real-world networks.

Notation. We say that sequence of events $\{\mathcal{E}_n\}$ occurs with high probability (w.h.p.) when $\lim_{n \rightarrow \infty} \mathbb{P}(\mathcal{E}_n) = 1$. We say that a sequence $\{X_n\}$ of random variables converges to the random variable X in probability, $X_n \xrightarrow{\mathbb{P}} X$, when $\lim_{n \rightarrow \infty} \mathbb{P}(|X_n - X| > \varepsilon) = 0$.

II. MODELS

In this paper, our benchmark model is the Geometric Inhomogeneous random graph [18], denoted by GIRG. This is a powerful, but tractable, random graph model that generalizes the hyperbolic random graph defined by Krioukov et al. in [2]. In the GIRG model, each vertex $i \in \{1, 2, \dots, n\}$ is equipped with a weight h_i and a uniformly sampled position x_i on a d -dimensional torus $[0, 1]^d$ endowed with the infinity norm. Weights are sampled independently from the Pareto distribution, with density

$$\rho(h) = K_1 h^{-\tau}, \quad (1)$$

for any $h > h_0 > 0$, where K_1 is the normalizing constant and $\tau \in (2, 3)$. Two nodes i and j , are then connected independently with probability

$$p(h_i, h_j, x_i, x_j) = K_2 \min \left(\frac{h_i h_j}{\mu n} \|x_i - x_j\|^{-d}, 1 \right)^\gamma, \quad (2)$$

for some $\gamma > 1$ and where μ denotes the average weight. The constant K_2 is a correction factor, which ensures that the expected degree of any vertex i is proportional to its weight h_i (see Appendix A).

In its original formulation, Bringmann et al. [3] defined the GIRG as an entire class of models, where the connection probability (2) is only required to hold asymptotically. Here we focus on a specific element of this class, to have a practical and tractable comparison with non-geometric models. An important reason to study the GIRG is that for $d = 1, \gamma = \infty$ it is asymptotically equivalent to the hyperbolic random graph, as shown in [18, 19]. Thus, the asymptotic results on the GIRG shown here are valid for the hyperbolic random graph as well.

To determine when geometry can be detected, we compare the GIRG to the Inhomogeneous random graph, which we denote by IRG. This model differs from the GIRG only in the sense that it is non-geometric. Specifically, the vertices now possess only weights h_i , sampled from the Pareto distribution as in (1), and are connected with probability

$$p(h_i, h_j) = \min \left(\frac{h_i h_j}{\mu n}, 1 \right). \quad (3)$$

The two models have the same weight, and degree distribution [20, 21], and differ only in their connection probability through the presence of geometry. We will therefore show that under classical triangle-based statistics, these models cannot be distinguished, making it impossible to distinguish hyperbolic geometry from simple scale-free networks.

III. TRIANGLE COUNTS

The most intuitive statistic to detect geometry is the triangle count in the network, Δ . Indeed, one would expect a high number of triangles in geometric networks due to the triangle inequality. The number of triangles in the IRG scales as $n^{3(3-\tau)/2}$ [22]. In the GIRG on the other hand, the triangle count undergoes a phase transition: when $\tau < 7/3$ it scales as $n^{3(3-\tau)/2}$, and when $\tau > 7/3$ it scales as n [17, 23, 24]. Then, for small values of τ , we cannot distinguish geometry from the triangle counts scaling, as in both models the number of triangles is proportional to $n^{3(3-\tau)/2}$. In Figures 1a and 1b we clearly see that when $\tau = 2.1$, the number of triangles in geometric and non-geometric models grow with the same scaling.

Theoretically, even when τ is small, it could still be possible to distinguish geometric/non-geometric inhomogeneous models through triangle counts. Indeed, if the number of triangles is $\Delta = A n^{3(3-\tau)/2} (1 + o(1))$, we may be able to establish the correct underlying model, by identifying the leading order term A . To this end, we can use precise asymptotic results from our earlier work [17, 22]:

In the IRG,

$$\frac{\Delta}{n^{3(3-\tau)/2}} \xrightarrow{\mathbb{P}} A_{\text{IRG}}.$$

In the GIRG, when $\tau < 7/3$,

$$\frac{\Delta}{n^{3(3-\tau)/2}} \xrightarrow{\mathbb{P}} A_{\text{GIRG}}.$$

Here, A_{IRG} and A_{GIRG} are explicit constants that depend on the parameters of the two models. If these are all known, then the two models could be distinguished using the difference between A_{IRG} and A_{GIRG} . However, in realistic situations, one observes a network only through its connections, while the possible underlying geometry

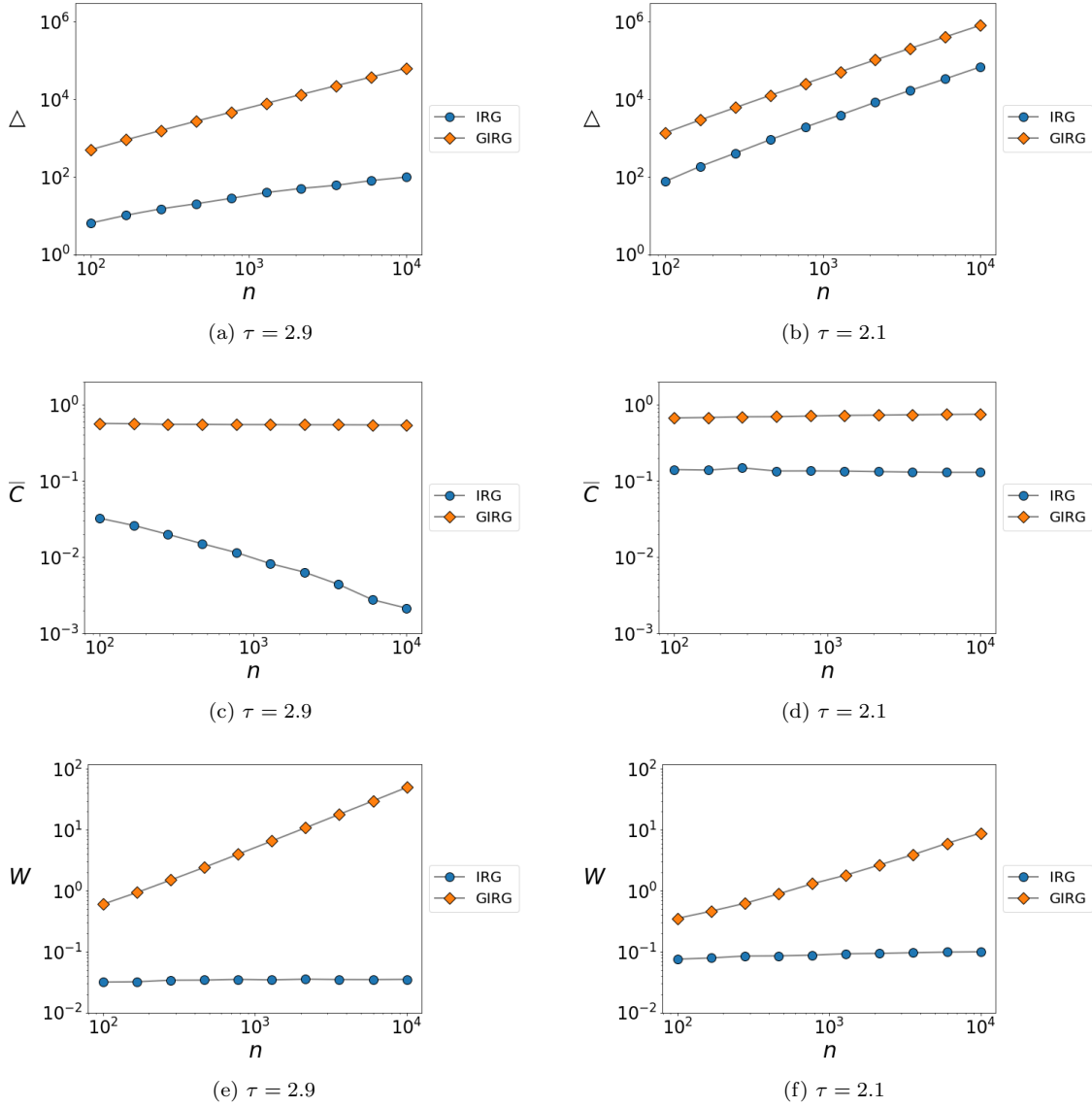


FIG. 1. Triangle counts, clustering coefficient and weighted triangles for the Inhomogeneous random graph (IRG) and Geometric Inhomogeneous random graph (GIRG). Dots are the averages over 100 samples of IRG and GIRG, against the number of vertices n . Grey lines are linear interpolations between dots. (a) When $\tau > 7/3$, the number of triangles increases linearly in GIRG, but slower than linearly for IRG. (b) When $\tau < 7/3$, the triangles in the non-geometric and geometric model share the same scaling. (c) When τ is large, \bar{C} differs significantly between the non-geometric and geometric model. (d) When τ is small, \bar{C} is qualitatively similar in both models. (e) (f) W is significantly different both for small and large values of τ . In particular, in non-geometric models W remains bounded below $1/6$.

of the network and the vertex weights are usually not known. Therefore, in practice, we cannot estimate the parameters of the underlying models, and thus it is impossible to establish whether the triangle count is close to $A_{\text{IRG}} n^{3(3-\tau)/2}$ or $A_{\text{GIRG}} n^{3(3-\tau)/2}$.

We conclude that the number of triangles is not a satisfactory statistic for inferring the hyperbolic geometry.

IV. AVERAGE CLUSTERING COEFFICIENT

Another common network statistic to measure the tendency of the nodes to form triangles, is the clustering coefficient, which has also been ascribed to indicate a network geometry [12].

The average clustering coefficient captures the probability that two randomly chosen neighbors of a randomly chosen vertex are connected as well. Equivalently, it is the average fraction of realized triangles out of all possi-

ble triangles that include a randomly chosen vertex:

$$\bar{C} = \frac{1}{n} \sum_{i \in V} C_i = \frac{1}{n} \sum_{i \in V} \frac{2\Delta_i}{d_i(d_i - 1)}, \quad (4)$$

where Δ_i is the number of triangles containing vertex i , and d_i is the degree of vertex i . Typically, if the value of \bar{C} does not vanish in n , then this is considered to be evidence for geometry.

The average clustering in GIRGs is non-vanishing as n increases [18]. In particular, in hyperbolic random graphs, \bar{C} converges in probability to a positive constant [25]. For the IRG on the other hand, \bar{C} decays asymptotically, as $n^{\tau-2} \ln(n)$ [26, 27]. Even though \bar{C} vanishes for large n , the decay of \bar{C} is extremely slow when $\tau \approx 2$, as we can observe in Figure 1c. Thus, the average clustering coefficient is impractical to detect geometry when τ is small.

Even more importantly, in non-geometric models with a different heavy-tailed degree distribution, \bar{C} can even be constant. For example, consider an inhomogeneous random graph with weights

$$h_i = \begin{cases} 2, & \text{with probability } 1 - 1/(\sqrt{\mu n}), \\ \sqrt{\mu n}, & \text{with probability } 1/(\sqrt{\mu n}). \end{cases}$$

We show in Appendix F that \bar{C} is constant in this IRG, even though the model does not contain any source of geometry. Hence, \bar{C} too, is not a good statistic to distinguish between geometric and non-geometric networks.

V. WEIGHTED TRIANGLES

We will now describe our proposed statistic that, contrary to standard clustering-based statistics, is able to detect hyperbolic geometry. This statistic is again triangle-based so that it has the same computational complexity as other clustering-based statistics. The difference between our statistic and the average clustering coefficient or triangle count, is that all triangles are weighted based on their evidence for geometry. Indeed, in a hyperbolic space, triangles can be formed because of popularity (high-degree vertices), or similarity (close-by vertices). Thus, we weigh each triangle, so that triangles which carry low evidence for geometry have low weight, and triangles which carry high evidence for being formed due to geometry have high weight. More precisely, we define the *weighted triangles* count

$$W := \sum_{\substack{i,j,k \in V \\ i < j < k}} \frac{1}{d_i d_j d_k} \mathbb{1}_{\{(i,j,k)=\Delta\}}, \quad (5)$$

where $\mathbb{1}_{\{(i,j,k)=\Delta\}}$ is the indicator function of the event that the vertices i, j, k form a triangle in the network. The intuition behind the weights $(d_i d_j d_k)^{-1}$ is that, in non-geometric power-law models, a typical triangle is

formed between vertices of high degrees [23]. Thus, when we *discount* the triangles formed by high-degree vertices, W remains small. On the other hand, in the GIRG, there is a large number of triangles formed by close-by vertices with small degrees. Therefore, W is significantly greater for GIRGs than for IRGs.

Indeed, as we show in Appendix E, w.h.p.,

$$\begin{aligned} W &\leq 1/6, \text{ in IRG,} \\ W &\geq \delta n, \text{ in GIRG,} \end{aligned}$$

for some $\delta > 0$. Thus, weighted triangles make a very powerful statistic to infer hyperbolic geometry: in the absence of geometry, the statistic remains bounded, while it scales at least linearly under a geometric model. Moreover, this different behaviour is independent of τ . This is clearly seen in Figures 1e and 1f, where W shows different scaling in non-geometric/geometric models, regardless of τ .

It is interesting to observe that the average clustering coefficient can be seen as a specific way of weighing triangles as well:

$$\begin{aligned} n\bar{C} &= \sum_{\substack{i,j,k \in V \\ i < j < k}} \left[\frac{1}{\binom{d_i}{2}} + \frac{1}{\binom{d_j}{2}} + \frac{1}{\binom{d_k}{2}} \right] \mathbb{1}_{\{(i,j,k)=\Delta\}} \\ &\approx n\bar{C}_h := \sum_{\substack{i,j,k \in V \\ i < j < k}} 2 \left(\frac{1}{h_i^2} + \frac{1}{h_j^2} + \frac{1}{h_k^2} \right) \mathbb{1}_{\{(i,j,k)=\Delta\}}. \end{aligned} \quad (6)$$

On the other hand,

$$W \approx W_h := \sum_{\substack{i,j,k \in V \\ i < j < k}} \frac{1}{h_i h_j h_k} \mathbb{1}_{\{(i,j,k)=\Delta\}}. \quad (7)$$

By [17, 23, 24], triangles containing high-weighted vertices are likely to appear in scale-free models regardless of the geometry of the system. Thus, an effective statistic for geometry detection should discount triangles formed by high-degree vertices. From (6) and (7) we see that such discounting occurs in both $n\bar{C}_h$ and W_h . However, in W_h , the factor $1/(h_i h_j h_k)$ is small as soon as *at least one* of the three vertices has high weight. On the contrary, in $n\bar{C}_h$, the factor $1/h_i^2 + 1/h_j^2 + 1/h_k^2$ is small if and only if *all three vertices* have high weights. Therefore, W discounts triangles formed by high-weight vertices more effectively than $n\bar{C}$ does. Indeed, Appendix F shows that the average clustering coefficient may also be constant for non-geometric networks, while weighted triangles are able to detect the non-geometric nature of the underlying network. This makes weighted triangles W a better geometry detector than the average clustering coefficient.

VI. REAL-WORLD NETWORKS

We will now investigate the performance of our statistic on real-world data. As our statistic was designed

to infer hyperbolic geometry, we focus only on networks with a heavy-tailed degree distribution. Furthermore, we investigate data sets that contain multiple snapshots of different sizes of the same network, to compare the theoretical scaling of W with the scaling found in the data. These networks are described in detail in Table I.

Figure 2 shows the behavior of triangle counts \triangle , the average clustering coefficient \overline{C} and weighted triangles W .

In all four data sets, W behaves roughly linearly in n , as our theoretical analysis predicts for geometric networks. The clustering coefficient as well as the pure triangle counts on the other hand, has more erratic behavior that is difficult to interpret. We will now discuss the results for each network in some more detail.

W grows linearly for the ArXiv collaboration networks (Figure 2a): this suggests that geometry is present in the network. This corresponds to an intuition that ArXiv collaborations have a natural geometric structure: researchers working in the same group, region, or country are more likely to write a paper together. Moreover, a collaboration between two researchers is more likely if they work on similar topics.

The average clustering coefficient \overline{C} is rather small for the CAIDA AS networks (Figure 2b), and it seems to be decreasing, as the network size increases. On the other hand, the weighted triangles show a linear growth, revealing a source of geometry, that, in fact, is consistent with the domain knowledge about this network. Indeed, interactions between autonomous systems occur through peering or transit. An important part of peer selection is the following: internet service providers (ISPs) have a set of *points-of-presence*, that are the locations where they have routers/servers and related equipment/personnel across the world. An ISP can peer with another ISP only at locations where both have a point-of-presence. Such location-dependent connectivity rules naturally suggest the presence of an implicit geometry in the network formation.

The Gnutella peer-to-peer networks (Figure 2c) show an extremely small average clustering coefficient, failing to detect geometry. On the contrary, the weighted triangles reveal geometry, as W increases linearly with the

network size. Indeed, it is reasonable to expect a geometric structure in this network because peer-to-peer file transfers are more likely between users who share similar interests. Then, we could construct an hidden metric space, by embedding users into this space according to their interests.

Finally, the linear growth of W for the Bitcoin transaction network (Figure 2d) suggests the presence of geometry in this network as well. This is consistent with intuition about the topology of the network: bitcoin transactions have been observed to occur more often between public-key addresses that have entered the network at a similar time [32].

Note that the Bitcoin transactions network data is a single network with time stamps on the transactions, while the other datasets consist of several snapshots over time. For the Bitcoin network, we therefore create the time-snapshots ourselves by subsampling: we take the induced subgraphs over vertices and edges that have appeared up to a given time. In particular, the experiment on the Bitcoin network demonstrates that our method can be applied also to temporal networks which consist of a single issue, if vertices or edges have time stamps.

Overall, the plots in Figure 2 suggest that weighted triangles can be an effective statistic to detect geometry in real-world networks.

VII. CONCLUSION AND DISCUSSION

In this paper we have analyzed in detail different methods to detect hyperbolic geometry in networks, when only the connections of the network are known. For theoretical purposes, we used the IRG and GIRG as benchmark models, on which we established analytical results. In both random graph models, the probability of connection depends on the popularity features of individuals vertices, expressed through their weights, so that the empirical degree distribution is power law with parameter τ . However, GIRG also models similarity of individuals, by locating the graph vertices randomly in a d -dimensional torus endowed with a metric.

First, we have established that triangle counts and the average clustering coefficient have serious limitations in detecting the presence of geometry when the degree distribution has a particular heavy tail (when $\tau < 7/3$). Using numerical simulations we confirmed these limitations, by comparing the number of triangles and the average clustering coefficient in different models.

Next, we have introduced a new statistic, weighted triangles W , that effectively discounts triangles formed by high degree vertices. The underlying intuition is that such triangles carry low evidence for geometry because they are common in power law networks with or without an underlying geometric space. Our main result states that W is a suitable statistic for detecting geometry, because, asymptotically in the network size, W remains bounded in IRGs, while it grows linearly in GIRGs.

TABLE I. Overview of the data sets. *ArXiv collab* collects coauthorships between scientists posting preprints on the Condensed Matter E-Print Archive, from 1999 to 2005 [28]; *CAIDA AS* contains the CAIDA autonomous systems relationship, from January 2004 to November 2007 [29]; *Gnutella p2p* collects all Gnutella peer-to-peer file sharing connections from August 2002 [30].

Name	# snapshots	avg. n per snapshot
ArXiv collab [28]	3	29437
CAIDA AS [29]	122	22550
Gnutella p2p [30]	8	22811
Bitcoin trans [31]	10	3728100

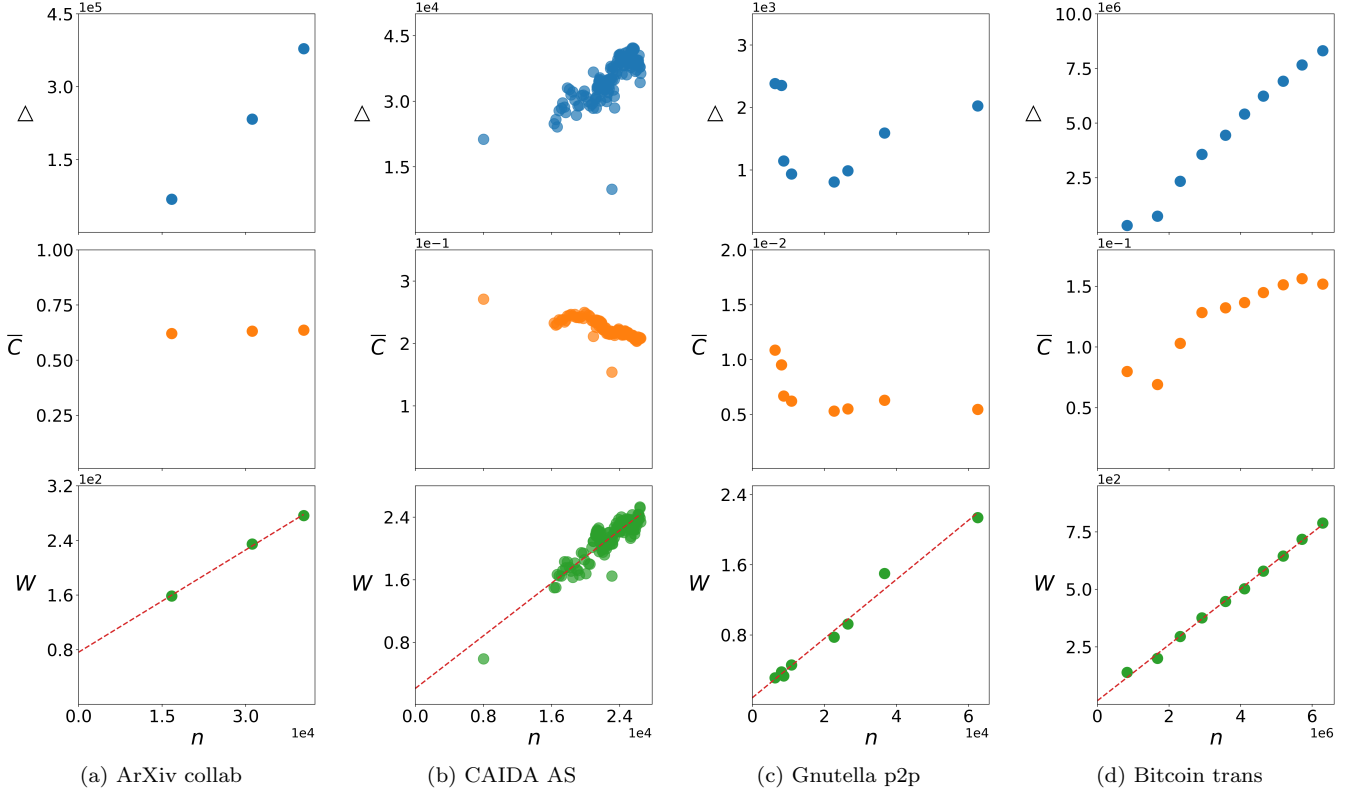


FIG. 2. Triangle counts Δ (blue), average clustering coefficient \bar{C} (orange), and weighted triangles W (green), computed for the data sets: (a) ArXiv collaboration (cond-mat); (b) CAIDA autonomous systems relationship; (c) Gnutella peer-to-peer connections; (d) Bitcoin transactions. The red line is the simple linear regression of W .

Numerical experiments on the real-world data show a remarkable agreement with this analysis, and confirm the high potential of the W statistic for uncovering a hidden network geometry.

We note that W scales linearly in all four real-life networks presented here. This raises the question whether there exist real-life networks in which W remains bounded. At this point, all non-bipartite real networks we have analyzed seem to possess hidden features which may produce geometric or community effects, such as positions, interests, locations or content similarity. The presence of such features in most real-life networks might explain why we have not found real-world networks with bounded W .

For practical applications, it would be interesting to know how large W should be to signal geometry. As in IRGs, $\mathbb{E}[W] \leq 1/6$ (Appendix B), Markov's inequality yields that

$$\mathbb{P}(W \geq n^\alpha) \leq \frac{1}{n^{\alpha-\varepsilon}} \rightarrow 0$$

for any $0 < \varepsilon < \alpha < 1$. On the other hand, in GIRGs, both $\mathbb{E}[W]$ and $\text{Var}[W]$ are linear in n (see Appendices C-D). Hence, Chebyshev's inequality gives

$$\mathbb{P}(W \leq n^\alpha) \rightarrow 0$$

in the large network limit. This means that n^α would work as a threshold for W to detect geometry, for any $\alpha \in (0, 1)$. However, even though W grows at least linearly in GIRGs, its leading order term can be small. For example, in Figure 2c, for $n = 50000$, W is still smaller than 2. Designing statistical tests for finite n is a natural next step, and one may expect that the use of W as test statistic needs to be accompanied by an estimate for the linear slope in GIRGs.

As a potential limitation, we remark that our statistic is designed specifically to distinguish the geometric GIRG and hyperbolic random graphs from their non-geometric counterparts. As such, it might not apply to other non-geometric models. For example, a *household model* [33] does not have an underlying geometry as in GIRG, but it does have many low-degree triangles within households. We thus believe that weighted triangles will grow linearly in this and other highly clustered non-geometric models. How to distinguish such models from models with underlying geometry, remains an open question.

Finally, the growth of W in n can be observed only in temporal networks or snapshots of networks. We illustrated that it is possible to give a rule of thumb on how large W should be to signal geometry in a single-snapshot network, but this procedure will depend on network parameters, such as degree exponents, that have to be esti-

mated first. Another possible approach is to artificially generate a series of snapshots of networks of different sizes through subsampling. Subsampling networks while preserving their properties is a difficult problem in itself, and is beyond the scope of this paper. In the future it will be interesting to apply weighted triangles to subsamples obtained, for example, by methods in randomized algorithms [34] or machine-learning [35].

Appendix A: Expected degree in GIRG

First, we introduce the asymptotic notation used in the Appendix. Let f, g be positive real functions defined on the natural numbers. We say that

- $f(n) = o(g(n))$ when $\lim_{n \rightarrow \infty} f(n)/g(n) = 0$;
- $f(n) = O(g(n))$ when $\limsup_{n \rightarrow \infty} f(n)/g(n) < \infty$;
- $f(n) = \Omega(g(n))$ when $\liminf_{n \rightarrow \infty} f(n)/g(n) > 0$,
- $f(n) = \Theta(g(n))$ when $f(n) = O(g(n))$ and $f(n) = \Omega(g(n))$.

We will also consistently use notation \mathbb{E}_y meaning that the averaging occurs with respect to random element y .

In this appendix, we calculate the expected degree of a vertex with weight h_i in a GIRG. First we show that in GIRGs the marginal connection probability, given the weight sequence (h_i) , is

$$\mathbb{E}_{x_i, x_j} [p(h_i, h_j, x_i, x_j)] = \Theta \left(\frac{h_i h_j}{n\mu} \wedge 1 \right),$$

where $a \wedge b := \min(a, b)$. Indeed, assuming that x_i is fixed and x_j is uniformly distributed, whence $\mathbb{P}(\|x_i - x_j\| \leq r) = \mathbb{P}(\|x_j\| \leq r)$, and denoting $V(r) = \mathbb{P}(\|x_j\| \leq r) = (2r)^d$, we obtain

$$\begin{aligned} \mathbb{E}_{x_j} [p(h_i, h_j, x_i, x_j)] &= \int_{[0,1]^d} K_2 \left[\frac{h_i h_j}{n\mu \|x_i - x_j\|^d} \wedge 1 \right]^\gamma dx_j \\ &= K_2 \int_0^{1/2} \left[\frac{h_i h_j}{n\mu r^d} \wedge 1 \right]^\gamma dV(r) \\ &= K_2 \int_0^{1/2} \left[\frac{h_i h_j 2^d}{n\mu V(r)} \wedge 1 \right]^\gamma dV(r). \end{aligned}$$

Then, averaging over x_i , and applying integral substitution, we get

$$\begin{aligned} \mathbb{E}_{x_i} [\mathbb{E}_{x_j} [p(h_i, h_j, x_i, x_j)]] &= \int_{[0,1]^d} \left(K_2 \int_0^1 \left[\frac{h_i h_j}{n\mu 2^{-d} V} \wedge 1 \right]^\gamma dV \right) dx_i \\ &= K_2 \int_0^1 \left[\frac{h_i h_j}{n\mu 2^{-d} V} \wedge 1 \right]^\gamma dV. \end{aligned}$$

Defining $r_0 := \frac{h_i h_j 2^d}{n\mu}$, consider the next two cases.

- If $r_0 \geq 1$, then the latter integrand is always 1. In such case we conclude $\mathbb{E}_{x_i, x_j} [p(h_i, h_j, x_i, x_j)] = 1$.
- If $r_0 < 1$, then

$$\begin{aligned} \mathbb{E}_{x_i, x_j} [p(h_i, h_j, x_i, x_j)] &= K_2 \left(\int_0^{r_0} 1 dV + \int_{r_0}^1 \left(\frac{r_0}{V} \right)^\gamma dV \right) \\ &= K_2 \left(r_0 + \left[\frac{r_0^\gamma}{\gamma - 1} (r_0^{-\gamma+1} - 1) \right] \right) \\ &= r_0 K_2 (1 + (\gamma - 1)^{-1}) + O(r_0^\gamma). \end{aligned}$$

Hence, setting the correction factor to the value $K_2 = (1 - \gamma^{-1})2^{-d}$,

$$\mathbb{E}_{x_i, x_j} [p(h_i, h_j, x_i, x_j)] = \begin{cases} 1, & \text{if } \frac{h_i h_j}{n} \geq \frac{\mu}{2^d}, \\ \frac{h_i h_j}{n\mu} + o\left(\frac{h_i h_j}{n\mu}\right), & \text{otherwise.} \end{cases} \quad (\text{A1})$$

Next, we can compute the marginal connection probability of the vertices i, j , only given the weight h_i . Substituting (1) and (A1), we obtain

$$\begin{aligned} \mathbb{E}_{h_j, x_i, x_j} [p(h_i, h_j, x_i, x_j)] &= \mathbb{E}_{h_j} [\mathbb{E}_{x_i, x_j} [p(h_i, h_j, x_i, x_j)]] \\ &\approx \int_{\frac{n\mu}{h_i 2^d}}^\infty K_1 h^{-\tau} dh \\ &\quad + \int_{h_0}^{\frac{n\mu}{h_i 2^d}} K_1 \frac{h_i}{n\mu} h^{-\tau+1} dh, \end{aligned}$$

where the approximation follows by dropping the lower order terms. Then:

$$\begin{aligned} \mathbb{E}_{h_j, x_i, x_j} [p(h_i, h_j, x_i, x_j)] &= K_1 \frac{h_i h_0^{2-\tau}}{n\mu(\tau-2)} + O((h_i/n)^{\tau-1}) \\ &= \frac{h_i}{n} (1 + o(1)), \end{aligned} \quad (\text{A2})$$

where the latter equality follows from the fact that $K_1 = (\tau-1)h_0^{\tau-1}$, $\mu = \frac{\tau-1}{\tau-2}h_0$. In other words, Equation (A2) tells that a vertex i with weight h_i connects to any other vertex with probability h_i/n , in the large n limit.

Finally, the expected degree of a vertex i with weight h_i is

$$\begin{aligned} \mathbb{E}[\deg(i)] &= \mathbb{E} \left[\sum_{j \neq i} \mathbb{1}_{\{(i \leftrightarrow j) | h_i\}} \right] \\ &= (n-1) \mathbb{E}_{h_j, x_i, x_j} [p(h_i, h_j, x_i, x_j)], \end{aligned}$$

and from Equation A2 we conclude that

$$\mathbb{E}[\deg(i)] \approx h_i.$$

Appendix B: Upper bound for $\mathbb{E}[W]$ in IRGs

The expected value of W in a IRG is given by

$$\mathbb{E}[W] = \sum_{i < j < k} \mathbb{E} \left[\frac{1}{d_i d_j d_k} \mathbb{1}_{\{(i,j,k)=\triangle\}} \right]. \quad (\text{B1})$$

To obtain the order of magnitude of (B1), we compute the upper bound of a similar quantity, where the degrees are replaced by the corresponding independent weights. In other words, $\mathbb{E}[W]$ is roughly approximated by

$$\begin{aligned} \mathbb{E}[W_h] &= \binom{n}{3} \int_{[h_0, \infty]^3} (h_1 h_2 h_3)^{-1} \prod_{1 \leq \alpha < \beta \leq 3} \left(\frac{h_\alpha h_\beta}{\mu n} \wedge 1 \right) \\ &\quad \times \rho(h_1) \rho(h_2) \rho(h_3) dh_1 dh_2 dh_3, \end{aligned}$$

where the binomial term arises from counting the possible combination of three vertices in V .

Since $\left(\frac{h_\alpha h_\beta}{\mu n} \wedge 1 \right) \leq \frac{h_\alpha h_\beta}{\mu n}$ for all α, β , the latter integral is upper bounded by

$$\left(\frac{K_1}{\mu n} \right)^3 \int_{[h_0, \infty]^3} (h_1 h_2 h_3)^{1-\tau} dh_1 dh_2 dh_3,$$

where K_1 is given by the Pareto power-law distribution for the weights. Then,

$$\begin{aligned} \mathbb{E}[W_h] &\leq \binom{n}{3} \left(\frac{K_1}{\mu n} \right)^3 \left(\int_{h_0}^{\infty} h^{1-\tau} dh \right)^3 \\ &= \binom{n}{3} \left(\frac{K_1}{\mu n} \right)^3 \left(\frac{h_0^{-\tau+2}}{\tau-2} \right)^3 \\ &= \binom{n}{3} \frac{1}{n^3} \leq \frac{1}{6}, \end{aligned}$$

where in the second equality we used the fact that $K_1/\mu = (\tau-2)h_0^{\tau-2}$. Since the degrees d_i in the IRG are concentrated around their means h_i , we conclude that $\mathbb{E}[W] = O(1)$.

Appendix C: Lower bound for $\mathbb{E}[W]$ in GIRGs

The expected value of W in GIRGs is

$$\mathbb{E}[W] = \sum_{i,j,k \in V} \mathbb{E} \left[\frac{1}{d_i d_j d_k} \mathbb{1}_{\{(i,j,k)=\triangle\}} \right]. \quad (\text{C1})$$

In a similar way as in Appendix B, to obtain the order of magnitude of (C1) we lower bound a similar quantity, where the degrees are replaced by the corresponding independent weights. That is, $\mathbb{E}[W]$ is roughly approximated by

$$\mathbb{E}[W_h] = \binom{n}{3} \int_{[h_0, \infty]^3} K_1^3 (h_1 h_2 h_3)^{-\tau-1} \int_{[0,1]^{3d}} \prod_{1 \leq \alpha < \beta \leq 3} K_2 \left(\frac{h_\alpha h_\beta}{\mu n \|x_\alpha - x_\beta\|^d} \wedge 1 \right)^\gamma dx_1 dx_2 dx_3 dh_1 dh_2 dh_3. \quad (\text{C2})$$

Observe that $\|x_2 - x_3\| \leq 2 \max\{\|x_1 - x_3\|, \|x_1 - x_2\|\}$ by the triangle inequality.

Then

$$\begin{aligned} \frac{1}{\|x_2 - x_3\|^d} &\geq \frac{1}{2^d \max\{\|x_1 - x_3\|^d, \|x_1 - x_2\|^d\}} \\ &= \left(\frac{1}{2^d \|x_1 - x_2\|^d} \wedge \frac{1}{2^d \|x_1 - x_3\|^d} \right). \end{aligned}$$

Substituting $(x_1, x_2, x_3) \rightarrow (z_1, z_2, z_3) := (x_1, x_2 - x_1, x_3 - x_1)$, the integral in (C2) is bounded from below

by

$$\begin{aligned} &\int_{[h_0, \infty]^3} K_1^3 (h_1 h_2 h_3)^{-\tau-1} \\ &\times K_2^3 \int_{[-1/2, 1/2]^{2d}} \left(\frac{h_2 h_3}{\mu n 2^d \|z_2\|^d} \wedge \frac{h_2 h_3}{\mu n 2^d \|z_3\|^d} \wedge 1 \right)^\gamma \\ &\times \left(\frac{h_1 h_2}{\mu n \|z_2\|^d} \wedge 1 \right)^\gamma \left(\frac{h_1 h_3}{\mu n \|z_3\|^d} \wedge 1 \right)^\gamma \\ &\times dz_2 dz_3 dh_1 dh_2 dh_3. \quad (\text{C3}) \end{aligned}$$

Now, consider the cube

$$\mathcal{C} := \left[-\left(\frac{h_0^2}{\mu n 2^d}\right)^{1/d}, \left(\frac{h_0^2}{\mu n 2^d}\right)^{1/d} \right]^d.$$

If $z_2 \in \mathcal{C}$ and $z_3 \in \mathcal{C}$, then all the minima in the integrand of (C3) are equal to 1. Therefore, after restricting the spatial integrals to the subset \mathcal{C}^2 , (C3) is lower bounded by

$$\int_{[h_0, \infty]^3} (K_1 K_2)^3 (h_1 h_2 h_3)^{-\tau-1} dh_1 dh_2 dh_3 \int_{\mathcal{C}^2} dz_2 dz_3.$$

Then, we obtain

$$\begin{aligned} \mathbb{E}[W_h] &\geq \binom{n}{3} \left(\int_{h_0}^{\infty} K_1 K_2 h^{-\tau-1} dh \right)^3 \left(\int_{\mathcal{C}^2} dz \right)^2 \\ &= \binom{n}{3} (K_1 K_2)^3 \frac{h_0^{3\tau}}{\tau^3} \left(\frac{h_0^2}{\mu n} \right)^2 \\ &= K_3 n (1 + o(1)), \end{aligned}$$

where K_3 is a non-null constant depending on the GIRG parameters τ, h_0, γ, d . Since the degrees d_i in the GIRG are concentrated around their means h_i , we conclude that $\mathbb{E}[W] = \Omega(n)$.

Appendix D: Upper bound for $\text{Var}[W]$ in GIRGs

Observe that

$$\begin{aligned} \text{Var}[W_h] &= \text{Var} \left[\sum_{i < j < k} \frac{\mathbb{1}_{\{i,j,k=\Delta\}}}{h_i h_j h_k} \right] \\ &= \sum_{\substack{i_1 < j_1 < k_1 \\ i_2 < j_2 < k_2}} \text{Cov} \left(\frac{\mathbb{1}_{\{i_1, j_1, k_1=\Delta\}}}{h_{i_1} h_{j_1} h_{k_1}}, \frac{\mathbb{1}_{\{i_2, j_2, k_2=\Delta\}}}{h_{i_2} h_{j_2} h_{k_2}} \right) \\ &\leq \sum_{\substack{i_1 < j_1 < k_1 \\ i_2 < j_2 < k_2}} \mathbb{E} \left[\frac{\mathbb{1}_{\{i_1, j_1, k_1=\Delta\}} \mathbb{1}_{\{i_2, j_2, k_2=\Delta\}}}{h_{i_1} h_{j_1} h_{k_1} h_{i_2} h_{j_2} h_{k_2}} \right] \\ &= \sum_{\substack{i_1 < j_1 < k_1 \\ i_2 < j_2 < k_2}} \mathbb{E}_{\bar{h}, \bar{x}} \left[\frac{\mathbb{P}(i_1, j_1, k_1 = \Delta) \mathbb{P}(i_2, j_2, k_2 = \Delta)}{h_{i_1} h_{j_1} h_{k_1} h_{i_2} h_{j_2} h_{k_2}} \right], \end{aligned} \tag{D1}$$

where indices \bar{h}, \bar{x} mean that the expectation is performed over all the random variables $(h_i)_{i \in [n]}$ and $(x_i)_{i \in [n]}$. There are now 4 different cases for the choices of $i_1, j_1, k_1, i_2, j_2, k_2$:

- (i) (i_1, j_1, k_1) and (i_2, j_2, k_2) do not intersect.

In this case the covariance is 0, because the two random variables $\frac{\mathbb{1}_{\{i_1, j_1, k_1=\Delta\}}}{h_{i_1} h_{j_1} h_{k_1}}$ and $\frac{\mathbb{1}_{\{i_2, j_2, k_2=\Delta\}}}{h_{i_2} h_{j_2} h_{k_2}}$ are independent.

- (ii) (i_1, j_1, k_1) and (i_2, j_2, k_2) intersect at 1 vertex (wlog $i_1 = i_2$). There are $O(n^5)$ ways to choose the vertices. We can bound the probabilities

$$\begin{aligned} \mathbb{P}(i_1, j_1, k_1 = \Delta) &\leq p(h_{i_1}, h_{j_1}, x_{i_1}, x_{j_1}) p(h_{j_1}, h_{k_1}, x_{j_1}, x_{k_1}) \\ \mathbb{P}(i_2, j_2, k_2 = \Delta) &\leq p(h_{i_2}, h_{j_2}, x_{i_2}, x_{j_2}) p(h_{j_2}, h_{k_2}, x_{j_2}, x_{k_2}) \end{aligned}$$

Moreover, for any sequence of nodes $(\alpha_1, \dots, \alpha_m)$,

$$\begin{aligned} \mathbb{E}_{\bar{x}} \left[\prod_{\ell=1}^{m-1} p(h_{\alpha_\ell}, h_{\alpha_{\ell+1}}, x_{\alpha_\ell}, x_{\alpha_{\ell+1}}) \right] \\ = \prod_{\ell=1}^{m-1} \mathbb{E}_{\bar{x}} [p(h_{\alpha_\ell}, h_{\alpha_{\ell+1}}, x_{\alpha_\ell}, x_{\alpha_{\ell+1}})]. \end{aligned}$$

This is a consequence of the fact that the positions are i.i.d. uniformly distributed in the torus, and that the connection probability is a function of the distance. Then, the terms in the sum of the r.h.s. in (D1) are upper bounded by

$$\begin{aligned} \mathbb{E}_{\bar{h}} \left[\frac{\mathbb{E}_{\bar{x}}[p(h_{k_1}, h_{j_1}, x_{k_1}, x_{j_1})] \mathbb{E}_{\bar{x}}[p(h_{j_1}, h_{i_1}, x_{j_1}, x_{i_1})] \mathbb{E}_{\bar{x}}[p(h_{i_1}, h_{j_2}, x_{i_1}, x_{j_2})] \mathbb{E}_{\bar{x}}[p(h_{j_2}, h_{k_2}, x_{j_2}, x_{k_2})]}{h_{i_1}^2 h_{j_1} h_{k_1} h_{j_2} h_{k_2}} \right] \\ = \int_{[h_0, \infty)^5} K_1^5 h_{i_1}^{-\tau-2} (h_{j_1} h_{k_1} h_{j_1} h_{k_2})^{-\tau-1} \frac{h_{k_1} h_{j_1}^2 h_{i_1}^2 h_{j_2}^2 h_{k_2}}{(n\mu)^4} dh_{i_1} dh_{j_1} dh_{k_1} dh_{j_2} dh_{k_2} = \frac{1}{n^4 \mu^2}. \end{aligned}$$

where the first equality follows from (A1). Then, the contribution to the variance from triangles overlapping in one vertex is $O(n^5/n^4) = O(n)$.

(iii) (i_1, j_1, k_1) and (i_2, j_2, k_2) do intersect in 2 vertices (wlog $i_1 = i_2, j_1 = j_2$). In this case the number of possible choices for the vertices is $O(n^4)$. We may bound the term in the r.h.s. of (D1) with

$$\begin{aligned} \mathbb{E}_h \left[\frac{\mathbb{E}_{\bar{x}}[p(h_{k_1}, h_{j_1}, x_{k_1 j_1})] \mathbb{E}_{\bar{x}}[p(h_{j_1}, h_{i_1}, x_{j_1 i_1})] \mathbb{E}_{\bar{x}}[p(h_{i_1}, h_{k_2}, x_{i_1 k_2})]}{h_{i_1}^2 h_{j_1}^2 h_{k_1} h_{k_2}} \right] \\ = \int_{[h_0, \infty)^4} K_1^4(h_{i_1} h_{j_1})^{-\tau-2} (h_{k_1} h_{k_2})^{-\tau-1} \frac{h_{k_1} h_{j_1}^2 h_{i_1}^2 h_{k_2}}{(n\mu)^3} dh_{i_1} dh_{j_1} dh_{k_1} dh_{k_2} = \frac{1}{n^3 \mu^3}, \end{aligned}$$

where the first equality follows from (A1). Then, the contribution to the variance from triangles overlapping in two vertices is $O(n^4/n^3) = O(n)$.

$(i_1 = i_2, j_1 = j_2, k_1 = k_2)$.

There are $\binom{n}{3}$ ways to choose the vertices. We upper bound the term in the r.h.s. of (D1) with

(iv) (i_1, j_1, k_1) and (i_2, j_2, k_2) intersect in 3 vertices

$$\mathbb{E}_h \left[\frac{\mathbb{E}_{\bar{x}}[p(h_{k_1}, h_{j_1}, x_{k_1 j_1})] \mathbb{E}_{\bar{x}}[p(h_{j_1}, h_{i_1}, x_{j_1 i_1})]}{h_{i_1}^2 h_{j_1}^2 h_{k_1}^2} \right] = \int_{[h_0, \infty)^3} K_1^3(h_{i_1} h_{j_1} h_{k_1})^{-\tau-2} \frac{h_{i_1} h_{j_1}^2 h_{k_1}}{(n\mu)^2} dh_{i_1} dh_{j_1} dh_{k_1} = \frac{1}{n^2} \left(\frac{\tau-2}{\tau h_0^2} \right)^2,$$

where, again, the first equality follows from (A1). Then, the contribution from triangles completely overlapping is $O(n)$.

such that $\mathbb{P}(W < \bar{\delta}n) < \varepsilon$, for all $n > n_0$. That is,

$$W = \Omega(n), \quad \text{with high probability.} \quad (\text{E3})$$

Appendix E: Concentration of W

Here we show that W concentrates around its expected value both in IRGs and in GIRGs.

In Appendix B we proved that $\mathbb{E}[W] = O(1)$, in IRGs. Then,

$$W = O(1), \quad \text{with high probability} \quad (\text{E1})$$

in IRG, as consequence of the Markov's inequality.

On the other hand, we proved that $\mathbb{E}[W] = \Omega(n)$ and $\text{Var}[W] = O(n)$ in GIRGs (Appendices C-D). By Chebyshev's inequality,

$$\mathbb{P} \left(\left| \frac{W}{\mathbb{E}[W]} - 1 \right| > \delta \right) \leq \frac{\text{Var}[W]}{\delta^2 \mathbb{E}[W]^2} = o(1), \quad (\text{E2})$$

for all $\delta > 0$. In particular, from Equation (E2) follows that, in GIRGs, for all $\varepsilon > 0$, there exist $\bar{\delta} > 0$, $n_0 > 0$

Appendix F: 2-type inhomogeneous model

Consider an inhomogeneous random graph where

$$h_i = \begin{cases} 2, & \text{with probability } 1 - 1/(\sqrt{\mu n}), \\ \sqrt{\mu n}, & \text{with probability } 1/(\sqrt{\mu n}). \end{cases}$$

We can approximate the weighted triangles W by

$$W_h = \sum_{i,j,k} \Delta_{i,j,k} (h_i h_j h_k)^{-1}.$$

Similarly, we can approximate the average clustering coefficient \bar{C} by

$$n\bar{C}_h = \sum_{i,j,k} \Delta_{i,j,k} (h_i^{-2} + h_j^{-2} + h_k^{-2}).$$

In this graph, a triangle falls into one of the four categories:

(I) The triangle has vertices with $h_i = h_j = h_k = 2$.

Each one of these triangles contributes

$$h_i^{-2} + h_j^{-2} + h_k^{-2} = 3/4$$

to \overline{C} , and

$$(h_i h_j h_k)^{-1} = 1/8$$

to W_h .

There are $O(n^3)$ sets containing 3 vertices of weight 2, and they form a triangle with probability

$$\begin{aligned} p(h_i, h_j)p(h_i, h_k)p(h_j, h_k) \\ = \left(\frac{4}{n\mu} \wedge 1\right) \left(\frac{4}{n\mu} \wedge 1\right) \left(\frac{4}{n\mu} \wedge 1\right) \\ = O(1/n^3). \end{aligned}$$

Thus, this triangle type contributes $O(1)$ to $n\overline{C}_h$, and $O(1)$ to W_h .

- (II) The triangle has $h_i = h_j = 2$, $h_k = \sqrt{\mu n}$. Each one of these triangles contributes

$$h_i^{-2} + h_j^{-2} + h_k^{-2} = \frac{1}{2} + \frac{1}{n\mu} \approx \frac{1}{2}$$

to \overline{C} , and

$$(h_i h_j h_k)^{-1} = \frac{1}{4\sqrt{n\mu}}$$

to W_h .

There are $\Theta(n^{5/2})$ sets containing 2 vertices of weight 2 and one with weight $\sqrt{\mu n}$, and they form a triangle with probability

$$\begin{aligned} p(h_i, h_j)p(h_i, h_k)p(h_j, h_k) \\ = \left(\frac{4}{n\mu} \wedge 1\right) \left(\frac{2}{\sqrt{n\mu}} \wedge 1\right) \left(\frac{2}{\sqrt{n\mu}} \wedge 1\right) \\ = \Theta(n^{-2}). \end{aligned}$$

Thus, this triangle type contributes $\Theta(\sqrt{n})$ to $n\overline{C}_h$, and $O(1)$ to W_h .

- (III) The triangle has $h_i = 2$, $h_j = h_k = \sqrt{\mu n}$. Each one of these triangles contributes

$$h_i^{-2} + h_j^{-2} + h_k^{-2} = \frac{1}{4} + \frac{2}{n\mu} \approx \frac{1}{4}$$

to \overline{C} , and

$$(h_i h_j h_k)^{-1} = \frac{1}{2n\mu}$$

to W_h .

There are $\Theta(n^2)$ sets containing of one vertex of

weight 2 and two with weight $\sqrt{\mu n}$, and they form a triangle with probability

$$\begin{aligned} p(h_i, h_j)p(h_i, h_k)p(h_j, h_k) \\ = \left(\frac{2}{\sqrt{n\mu}} \wedge 1\right) \left(\frac{2}{\sqrt{n\mu}} \wedge 1\right) \\ = \Theta(n^{-1}). \end{aligned}$$

Thus, this triangle type contributes $\Theta(n)$ to $n\overline{C}_h$, and $O(1)$ to W_h .

- (IV) The triangle has $h_i = h_j = h_k = \sqrt{\mu n}$. Each one of these triangles contributes

$$h_i^{-2} + h_j^{-2} + h_k^{-2} = \frac{3}{n\mu}$$

to \overline{C} , and

$$(h_i h_j h_k)^{-1} = \frac{1}{(n\mu)^3/2}$$

to W_h .

There are $\Theta(n^{3/2})$ sets containing three vertices with weight $\sqrt{\mu n}$, and they form a triangle with probability

$$p(h_i, h_j)p(h_i, h_k)p(h_j, h_k) = 1.$$

Thus, this triangle type contributes $\Theta(\sqrt{n})$ to $n\overline{C}_h$, and $O(1)$ to W_h .

Thus the total contributions to $n\overline{C}$ are:

- $O(1)$, from type (I) triangles;
- $\Theta(\sqrt{n})$, from type (II) triangles;
- $\Theta(n)$, from type (III) triangles;
- $\Theta(\sqrt{n})$, from type (IV) triangles.

Hence, $n\overline{C}_h = \Theta(n)$.

On the other hand, the total contributions to W are:

- $O(1)$, from type (I) triangles;
- $\Theta(1)$, from type (II) triangles;
- $\Theta(1)$, from type (III) triangles;
- $\Theta(1)$, from type (IV) triangles.

Hence, $W_h = \Theta(1)$.

[1] M. Boguñá, I. Bonamassa, M. D. Domenico, S. Havlin, D. Krioukov, and M. Á. Serrano, Network geometry, Na-

ture Reviews Physics **3**, 114 (2021).

[2] D. Krioukov, F. Papadopoulos, M. Kitsak, A. Vahdat,

- and M. Boguná, Hyperbolic geometry of complex networks, *Phys. Rev. E* **82**, 036106 (2010).
- [3] K. Bringmann, R. Keusch, and J. Lengler, Average distance in a general class of scale-free networks with underlying geometry, *arXiv preprint arXiv:1602.05712* (2018).
 - [4] M. Deijfen, R. Van der Hofstad, and G. Hooghiemstra, Scale-free percolation, in *Annales de l'IHP Probabilités et statistiques*, Vol. 49 (2013) pp. 817–838.
 - [5] M. A. Serrano, D. Krioukov, and M. Boguná, Self-similarity of complex networks and hidden metric spaces, *Phys. Rev. Lett.* **100**, 078701 (2008).
 - [6] M. Penrose *et al.*, *Random geometric graphs*, Vol. 5 (Oxford university press, 2003).
 - [7] J. Dall and M. Christensen, Random geometric graphs, *Physical review E* **66**, 016121 (2002).
 - [8] T. Bläsius, C. Freiberger, T. Friedrich, M. Katzmann, F. Montenegro-Retana, and M. Thieffry, Efficient shortest paths in scale-free networks with underlying hyperbolic geometry, in *International Colloquium on Automata, Languages, and Programming (ICALP)*, Vol. 107 (2018) pp. 20:1–20:14.
 - [9] R. Kleinberg, Geographic routing using hyperbolic space, in *IEEE INFOCOM 2007 - 26th IEEE International Conference on Computer Communications* (IEEE, 2007).
 - [10] A. Faqeeh, S. Osat, and F. Radicchi, Characterizing the analogy between hyperbolic embedding and community structure of complex networks, *Phys. Rev. Lett.* **121**, 098301 (2018).
 - [11] A. L. Smith, D. M. Asta, and C. A. Calder, The geometry of continuous latent space models for network data, *Statistical science: a review journal of the Institute of Mathematical Statistics* **34**, 428 (2019).
 - [12] D. Krioukov, Clustering implies geometry in networks, *Phys. Rev. Lett.* **116**, 208302 (2016).
 - [13] L. Devroye, A. György, G. Lugosi, and F. Udina, High-Dimensional Random Geometric Graphs and their Clique Number, *Electronic Journal of Probability* **16**, 2481 (2011).
 - [14] C. Gao and J. Lafferty, Testing for global network structure using small subgraph statistics, *arXiv preprint arXiv:1710.00862* (2017).
 - [15] S. Bubeck, J. Ding, R. Eldan, and M. Z. Rácz, Testing for high-dimensional geometry in random graphs, *Random Structures & Algorithms* **49**, 503 (2016).
 - [16] J. van der Kolk, M. Ángeles Serrano, and M. Boguná, A geometry-induced topological phase transition in random graphs, *arXiv preprint arXiv:2106.08030v2* (2022).
 - [17] R. Michielan and C. Stegehuis, Cliques in geometric inhomogeneous random graphs, *Journal of Complex Networks* **10** (2022).
 - [18] K. Bringmann, R. Keusch, and J. Lengler, Geometric inhomogeneous random graphs, *Theoretical Computer Science* **760**, 35 (2019).
 - [19] J. Komjáthy and B. Lodewijks, Explosion in weighted hyperbolic random graphs and geometric inhomogeneous random graphs, *Stochastic Processes and their Applications* **130**, 1309 (2020).
 - [20] B. Bollobás, S. Janson, and O. Riordan, The phase transition in inhomogeneous random graphs, *Random Structures & Algorithms* **31**, 3 (2007).
 - [21] R. Hofstad, P. van der Hoorn, and N. Maitra, Local limits of spatial inhomogeneous random graphs, *arXiv preprint arXiv:2107.08733* (2021).
 - [22] C. Stegehuis, R. van der Hofstad, and J. S. van Leeuwen, Variational principle for scale-free network motifs, *Scientific reports* **9**, 1 (2019).
 - [23] R. van der Hofstad, J. S. H. van Leeuwen, and C. Stegehuis, Optimal subgraph structures in scale-free configuration models, *The Annals of Applied Probability* **31**, 501 (2021).
 - [24] T. Bläsius, T. Friedrich, and A. Krohmer, Cliques in hyperbolic random graphs, *Algorithmica* **80**, 2324 (2018).
 - [25] N. Fountoulakis, P. Van Der Hoorn, T. Müller, and M. Schepers, Clustering in a hyperbolic model of complex networks, *Electronic Journal of Probability* **26** (2021).
 - [26] P. Colomer-de Simon and M. Boguná, Clustering of random scale-free networks, *Phys. Rev. E* **86**, 026120 (2012).
 - [27] R. van der Hofstad, A. J. E. M. Janssen, J. S. H. van Leeuwen, and C. Stegehuis, Local clustering in scale-free networks with hidden variables, *Phys. Rev. E* **95**, 10.1103/PhysRevE.95.022307 (2017).
 - [28] M. E. Newman, The structure of scientific collaboration networks, *Proceedings of the National Academy of Sciences of the United States of America* **98**, 404 (2001).
 - [29] The CAIDA AS Relationships Dataset (January 2004 to November 2007) .
 - [30] R. Matei, A. Iamnitchi, and P. Foster, Mapping the gnutella network, *IEEE Internet Computing* **6**, 50 (2002).
 - [31] The Bitcoin network (January 2009 to April 2013) .
 - [32] M. Fire and C. Guestrin, The rise and fall of network stars: Analyzing 2.5 million graphs to reveal how high-degree vertices emerge over time, *Information Processing & Management* **57**, 102041 (2020).
 - [33] J. Ma, P. van den Driessche, and F. H. Willeboordse, Effective degree household network disease model, *Journal of mathematical biology* **66**, 75 (2013).
 - [34] P. Orbanz, Testing for global network structure using small subgraph statistics, *arXiv preprint arXiv:1710.04217v1* (2017).
 - [35] A. Bojchevski, O. Shchur, D. Zügner, and S. Günnemann, NetGAN: Generating graphs via random walks, in *Proceedings of the 35th International Conference on Machine Learning*, *Proceedings of Machine Learning Research*, Vol. 80, edited by J. Dy and A. Krause (PMLR, 2018) pp. 610–619.